Chapter 13

Rate-Adaptive Free-Space Optical Links Over Atmospheric Turbulence and Misalignment Fading Channels

Antonio García-Zambrana, Carmen Castillo-Vázquez and Beatriz Castillo-Vázquez

Additional information is available at the end of the chapter

http://dx.doi.org/10.5772/45783

1. Introduction

Atmospheric free-space optical (FSO) transmission using intensity modulation and direct detection (IM/DD) can provide high-speed links for a variety of applications, being an interesting alternative to consider for next generation broadband in order to support large bandwidth, unlicensed spectrum, excellent security, and quick and inexpensive setup [9]. Recently, the use of FSO transmission is being specially interesting to solve the *"last mile" problem*, as well as a supplement to radio-frequency (RF) links [35, 41]. However, atmospheric turbulence produces fluctuations in the irradiance of the transmitted optical beam, which is known as *atmospheric scintillation*, severely degrading the link performance [3, 50]. Additionally, since FSO systems are usually installed on high buildings, building sway causes vibrations in the transmitted beam, leading to an unsuitable alignment between transmitter and receiver and, hence, a greater deterioration in performance.

Error control coding as well as diversity techniques can be used over FSO links to mitigate turbulence-induced fading [6, 7, 13, 33, 44]. In [20, 24, 26], selection transmit diversity is proposed for FSO links over strong turbulence channels, where the transmit diversity technique based on the selection of the optical path with a greater value of irradiance has shown to be able to extract full diversity as well as providing better performance compared to general FSO space-time codes (STCs) designs, such as conventional orthogonal space-time block codes (OSTBCs) and repetition codes (RCs). The combined effect of atmospheric and misalignment fading is analyzed in the case of single-input/single-output (SISO) FSO channels in [5]. In [16], the effects of atmospheric turbulence and misalignment considering aperture average effect were considered to study the outage capacity for SISO links. In [38] the error rate performance for coded FSO links over strong turbulence and misalignment fading channels is studied. The capacity calculation and the analysis of error rate performance for FSO links over log-normal and gamma-gamma turbulence and misalignment fading channels is presented in [8] using a wave optics based approach. In [18, 39], a wide range of turbulence conditions with gamma-gamma atmospheric turbulence and pointing

errors is also considered on terrestrial FSO links, deriving closed-form expressions for the error-rate performance in terms of Meijer's G-functions. In [36], average capacity optimization is considered in this same context by numerically solving the derivative of the corresponding capacity expression, also mathematically treated as a Meijer's G-function. In [17], the study of the outage probability and diversity gain has been considered for multiple-input/multiple-output (MIMO) FSO communication systems impaired by log-normal atmospheric turbulence and misalignment fading, assuming repetition coding on the transmitter side and equal gain combining on the receiver side and showing that the diversity gain is conditioned only by misalignment parameters. In [21, 25], comparing different diversity techniques, a significant improvement in terms of outage and error-rate performance is demonstrated when MIMO FSO links based on transmit laser selection are adopted in the context of wide range of turbulence conditions (weak to strong), showing that better performance is achieved when increasing the number of transmit apertures instead of the number of receive apertures in order to guarantee a same diversity order.

An alternative approach to improving the performance in this turbulence FSO scenario is the employment of rate-adaptive transmission in order to make suitable the communication to the adverse channel conditions, depending on the available signal-to-noise ratio (SNR) until a sufficiently low error probability can be attained. Various FSO systems using adaptive modulation have been proposed [10, 12, 14, 34]. In [34], a variable rate FSO system employing adaptive Turbo-based coding schemes with on-off keying (OOK) formats was investigated. In [12, 14], an adaptive transmission scheme that varied both the power and the modulation order of a FSO system with M-ary pulse amplitude modulation (MPAM) has been studied. In [10], an adaptive transmission technique employing subcarrier phase shift keying (S-PSK) intensity modulation has been proposed. Another solution is the employment of adaptive transmission based on repetition coding, a well known technique employed in RF systems [2]. Based on the concept of temporal-domain diversity reception (TD-DR), this idea has been applied for FSO links in [32, 42, 43], where two separate channels over the same transmit and receive path are implemented. Both channels carry the same data, but one of the channels is delayed by the expected fade duration. In [23], a new and simple rate-adaptive transmission scheme for FSO communication systems with intensity modulation and direct detection over atmospheric turbulence channels is analyzed. This scheme is based on the joint use of repetition coding and variable silence periods, exploiting the potential time-diversity order (TDO) available in the turbulent channel as well as allowing the increase of the peak-to-average optical power ratio (PAOPR), which has shown to be a favorable characteristic in IM/DD FSO links [19, 24, 26].

In this chapter, this approach is extended to FSO communication systems using IM/DD over atmospheric turbulence channels with pointing errors. Novel closed-form asymptotic expressions are derived when the irradiance of the transmitted optical beam is susceptible to either a wide range of turbulence conditions (weak to strong), following a gamma-gamma distribution of parameters α and β, or pointing errors, following a misalignment fading model, as in [16–18, 38], where the effect of beam width, detector size and jitter variance is considered. Obtained results provide significant insight into the impact of various system and channel parameters, showing that the time-diversity order that can be fully exploited is independent of the pointing error when the equivalent beam radius at the receiver is at least $2(\min\{\alpha, \beta\})^{1/2}$ times the value of the pointing error displacement standard deviation at the receiver. In this fashion, the same slope of the bit-error rate (BER) performance versus average SNR as in a similar FSO scenario without pointing errors is corroborated. However, different coding gain,

i.e. the horizontal shift in the BER performance in the limit of large SNR, is achieved as a consequence of the severity of the pointing error effects and turbulence conditions. Here, not only rectangular pulses are considered but also on-off keying (OOK) formats with any pulse shape, corroborating the advantage of using pulses with high PAOPR. Moreover, since proper FSO transmission requires transmitters with accurate control of their beamwidth, asymptotic expressions are used to find the optimum beamwidth that minimizes the BER at different turbulence conditions. Simulation results are further demonstrated to confirm the accuracy and usefulness of the derived results, showing that asymptotic expressions here obtained lead to simple bounds on the bit error probability that get tighter over a wider range of SNR as the turbulence strength increases.

2. System and channel model

The use of infrared technologies based on IM/DD links is considered, where the instantaneous current in the receiving photodetector, $y(t)$, assumed to be ideal noncoherent (direct-detection) receiver can be written as

$$y(t) = \eta i(t) x(t) + z(t) \tag{1}$$

where η is the detector responsivity, assumed hereinafter to be the unity, $X \triangleq x(t)$ represents the optical power supplied by the source, assumed to be intensity-modulated, and $I \triangleq i(t)$ the equivalent real-valued fading gain (irradiance) through the optical channel between the laser and the receive aperture; $Z \triangleq z(t)$ is assumed to include any front-end receiver thermal noise as well as shot noise caused by ambient light much stronger than the desired signal at detector. In this case, the noise can usually be modeled to high accuracy as AWGN with zero mean and variance $N_0/2$, i.e. $Z \sim N(0, N_0/2)$, independent of the on/off state of the received bit [31]. Since the transmitted signal is an intensity, X must satisfy $\forall t\, x(t) \geq 0$. Due to eye and skin safety regulations, the average optical power is limited and, hence, the average amplitude of X is limited. Although limits are placed on both the average and peak optical power transmitted, in the case of most practical modulated optical sources, it is the average optical power constraint that dominates [30]. The received electrical signal $Y \triangleq y(t)$, however, can assume negative amplitude values. We use Y, X, I and Z to denote random variables and $y(t)$, $x(t)$, $i(t)$ and $z(t)$ their corresponding realizations. In this fashion, the atmospheric turbulence channel model consists of a multiplicative noise model, where the optical signal is multiplied by the channel irradiance.

We consider OOK formats with any pulse shape and reduced duty cycle, allowing the increase of the PAOPR parameter [19, 26]. In spite of the atmosphere can cause pulse distortion and broadening during propagation at extremely high signalling rates and, especially, at high levels of turbulence strength when increasing either C_n^2 or the path length L, or both, pulse shape distortion is assumed to be negligible for the typical FSO scenario here analyzed [15, 49]. A new basis function $\phi(t)$ is defined as $\phi(t) = g(t)/\sqrt{E_g}$ where $g(t)$ represents any normalized pulse shape satisfying the non-negativity constraint, with $0 \leq g(t) \leq 1$ in the bit period and 0 otherwise, and $E_g = \int_{-\infty}^{\infty} g^2(t)dt$ is the electrical energy. In this way, an expression for the optical intensity can be written as

$$x(t) = \sum_{k=-\infty}^{\infty} a_k \frac{2T_b P}{G(f=0)} g\left(t - kT_b\right) \tag{2}$$

where $G(f=0)$ represents the Fourier transform of $g(t)$ evaluated at frequency $f=0$, i.e. the area of the employed pulse shape, and T_b parameter is the bit period. The random variable (RV) a_k follows a Bernoulli distribution with parameter $p = 1/2$, taking the values of 0 for the bit "0" (off pulse) and 1 for the bit "1" (on pulse). From this expression, it is easy to deduce that the average optical power transmitted is P, defining a constellation of two equiprobable points in a one-dimensional space with an Euclidean distance of $d = 2P\sqrt{T_b\xi}$ where $\xi = T_b E_g / G^2(f=0)$ represents the square of the increment in Euclidean distance due to the use of a pulse shape of high PAOPR, alternative to the classical rectangular pulse.

Since atmospheric scintillation is a slow time varying process relative to typical symbol rates of an FSO system, having a coherence time on the order of milliseconds, we consider the time variations according to the theoretical block-fading model, where the channel fade remains constant during a block (corresponding to the channel coherence interval) and changes to a new independent value from one block to next. In other words, channel fades are assumed to be independent and identically distributed (i.i.d.). This temporal correlation can be overcome by means of long interleavers, being usually assumed both in the analysis from the point of view of information theory and error rate performance analysis of coded FSO links [4, 37, 45]. However, as in [48], we here assume that the interleaver depth can not be infinite and, hence, we can potentially benefit from a degree of time diversity limited equal to TDO. This consideration is justified from the fact that the latency introduced by the interleaver is not an inconvenience for the required application. For example, for repetition coding and a time diversity order available of TDO=2, i.e. two channel fades i_1 and i_2 per frame, perfect interleaving can be done by simply sending the same information delayed by the expected fade duration, as shown experimentally in [32] for a rate reduction of 2. In this system model, shown in Fig. 1, it is assumed that channel state information (CSI) is known

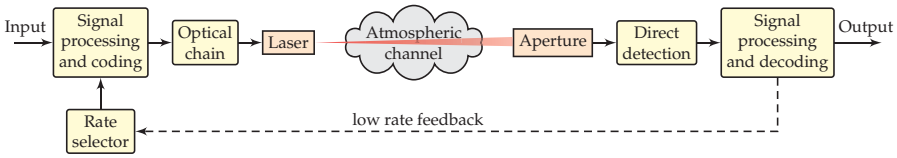

Figure 1. FSO system with rate-adaptive transmission.

not only at the receiver but also at the transmitter (CSIT). The knowledge of CSIT is feasible for FSO channels given that scintillation is a slow time varying process relative to the large symbol rate. Adaptive transmission here considered is based on reducing the initial bit rate, $R_b = 1/T_b$, for a rate reduction (RR) parameter as R_b/RR in order to satisfy a predefined BER requirement.

2.1. Proposed rate-adaptive transmission scheme

In this subsection, we firstly explain the case corresponding to the rate-adaptive transmission only based on variable silence periods; secondly, we present the case corresponding to the rate-adaptive transmission only based on repetition coding and, finally, we consider the adaptive transmission scheme here proposed and based on the joint use of repetition coding and variable silence periods, exploiting the potential time-diversity order available in the turbulent channel as well as allowing the increase of the PAOPR, which has shown to be a favorable characteristic in IM/DD links.

A rate-adaptive transmission scheme based on variable silence periods has already been proposed in [28] for indoor optical wireless communication systems as a consequence of the good performance of signaling techniques having a reduced duty cycle [27] and, hence, providing a high PAOPR. The advantage of using pulses with high PAOPR has also been corroborated in FSO links over atmospheric turbulence channels by closed-form expressions corresponding to the average BER performance [19, 24, 26], suggesting its application to the turbulent FSO scenario. A similar expression to (2) for the optical intensity corresponding to this adaptive technique only based on variable silence periods can be written as

$$x_{RR_s}(t) = \sum_{k=-\infty}^{\infty} a_k \frac{RR_s 2T_b P}{G(f=0)} g\left(t - kRR_s T_b\right) \tag{3}$$

where $RR_s - 1$ is the number of silence bit periods added in order to accomodate the transmission rate to the channel conditions, so that the higher rate reduction ($RR = RR_s$), the larger silence time. From this expression, it is easy to deduce that an increase of the PAOPR is required in order to maintain the average optical power at the same constant level of P.

In relation to the rate-adaptive transmission only based on repetition coding, the expression for the optical intensity can be written as

$$x_{RR_{rc}}(t) = \sum_{k=-\infty}^{\infty} a_k \frac{2T_b P}{G(f=0)} \sum_{l=0}^{RR_{rc}-1} g\left(t - lT_b - kRR_{rc} T_b\right) \tag{4}$$

where RR_{rc} represents the repetition of each information bit and, hence, a rate reduction of $RR = RR_{rc}$ is considered. From this expression, it is easy to deduce that an increase of the PAOPR is not achieved; however, unlike rate-adaptive transmission only based on variable silence periods, a potential diversity gain can be exploited based on the concept of temporal-domain diversity reception [32]. To the best of the authors' knowledge, closed-form expressions for the error rate performance corresponding to this rate-adaptive scheme in the context proper to FSO systems over atmospheric turbulence channels with pointing errors where a limited time-diversity order is only available have not been reported in the open literature.

Next, we combine the best of previous approaches, proposing a novel adaptive transmission scheme based on the joint use of repetition coding and variable silence periods and, this way, exploiting the potential time-diversity order available in the turbulent channel as well as allowing the increase of the PAOPR. In this fashion, the expression for the optical intensity can be written as

$$x_{RR_{rcs}}(t) = \sum_{k=-\infty}^{\infty} a_k \frac{RR_s 2T_b P}{G(f=0)} \sum_{l=0}^{RR_{rc}-1} g\left(t - lRR_s T_b - kRRT_b\right) \tag{5}$$

where the final rate reduction $RR = RR_{rc} \cdot RR_s$. In this adaptive transmission technique, repetition coding is firstly used in order to accomodate the transmission rate to the channel conditions until the whole time diversity order available in the turbulent channel by interleaving is exploited, i.e. $RR_{rc} \leq$ TDO and $RR_s = 1$. Then, once no more diversity gain is available, the rate reduction can be increased by using variable silence periods in order to increase the PAOPR, i.e. $RR_{rc} =$ TDO and $RR_s > 1$. For the sake of simplicity, we here consider values multiples of 2 for RR when rate reduction is applied, i.e $RR = \{1, 2, 4, 8, \cdots\}$

as well as for the time-diversity order effective TDO which is provided by interleaving, i.e. TDO $= \{1, 2, 4\}$, in this fashion, allowing to satisfy different latency requirements in the system [48].

2.2. Atmospheric turbulence channel

The irradiance is susceptible to either atmospheric turbulence conditions and pointing error effects. In this case, it is considered to be a product of two independent random variables, i.e. $I = I^{(a)} I^{(p)}$, representing $I^{(a)}$ and $I^{(p)}$ the attenuation due to atmospheric turbulence and the attenuation due to geometric spread and pointing errors, respectively, between transmitter and receiver. Although the effects of turbulence and pointing are not strictly independent, for smaller jitter values they can be approximated as independent [8]. To consider a wide range of turbulence conditions (weak to strong), the gamma-gamma turbulence model proposed in [1, 3] is here assumed, whose probability density function (PDF) is given by

$$f_{I^{(a)}}(i) = \frac{2(\alpha\beta)^{(\alpha+\beta)/2}}{\Gamma(\alpha)\Gamma(\beta)} i^{((\alpha+\beta)/2)-1} K_{\alpha-\beta}\left(2\sqrt{\alpha\beta i}\right), \quad i \geq 0 \tag{6}$$

where $\Gamma(\cdot)$ is the well-known Gamma function and $K_\nu(\cdot)$ is the νth-order modified Bessel function of the second kind [29, eqn. (8.43)]. The parameters α and β can be selected to achieve a good agreement between Eq. (6) and measurement data [1]. Alternatively, assuming spherical wave propagation, α and β can be directly linked to physical parameters through the following expresions [1, 7, 45]:

$$\alpha = \left[\exp\left(\frac{0.49\chi^2}{(1 + 0.18d^2 + 0.56\chi^{12/5})^{7/6}}\right) - 1\right]^{-1} \tag{7}$$

$$\beta = \left[\exp\left(\frac{0.51\chi^2(1 + 0.69\chi^{12/5})^{-5/6}}{(1 + 0.9d^2 + 0.62d^2\chi^{12/5})^{7/6}}\right) - 1\right]^{-1} \tag{8}$$

where $\chi^2 = 0.5C_n^2 k^{7/6} L^{11/6}$ and $d = (kD^2/4L)^{1/2}$. Here, $k = 2\pi/\lambda$ is the optical wave number, λ is the wavelength, D is the diameter of the receiver collecting lens aperture and L is the link distance in meters. C_n^2 stands for the altitude-dependent index of the refractive structure parameter and varies from 10^{-13} $m^{-2/3}$ for strong turbulence to 10^{-17} $m^{-2/3}$ for weak turbulence [3, 45]. Since the mean value of this turbulence model here considered is normalized and the second moment is given by $E[I^2] = (1 + 1/\alpha)(1 + 1/\beta)$, the scintillation index (SI), a parameter of interest used to describe the strength of atmospheric fading, is defined as

$$SI = \frac{E[I^2]}{(E[I])^2} - 1 = \frac{1}{\alpha} + \frac{1}{\beta} + \frac{1}{\alpha\beta}. \tag{9}$$

It must be noted that PDF in Eq. (6) contains other turbulence models adopted in strong turbulence FSO scenarios such as the K-distribution ($\beta = 1$ and $\alpha > 0$) and the negative exponential distribution ($\beta = 1$ and $\alpha \to \infty$) [20, 38, 44]. From the point of view of scintillation index, it is easy to deduce the fact that the strength of atmospheric fading represented by the gamma-gamma distributed turbulence model with channel parameters $\beta = 1$ and increasing α tends to be closer and closer to 1, SI corresponding to the negative exponential distributed

turbulence model. Regarding to the impact of pointing errors, we use the general model of misalignment fading given in [16] by Farid and Hranilovic, wherein the effect of beam width, detector size and jitter variance is considered. Assuming a Gaussian spatial intensity profile of beam waist radius, ω_z, on the receiver plane at distance z from the transmitter and a circular receive aperture of radius r, the PDF of $I^{(p)}$ is given by

$$f_{I^{(p)}}(i) = \frac{\varphi^2}{A_0^{\varphi^2}} i^{\varphi^2-1}, \quad 0 \le i \le A_0 \tag{10}$$

where $\varphi = \omega_{z_{eq}}/2\sigma_s$ is the ratio between the equivalent beam radius at the receiver and the pointing error displacement standard deviation (jitter) at the receiver, $v = \sqrt{\pi}r/\sqrt{2}\omega_z$, $\omega_{z_{eq}}^2 = \omega_z^2\sqrt{\pi}\mathrm{erf}(v)/2v\exp(-v^2)$, $A_0 = [\mathrm{erf}(v)]^2$ and $\mathrm{erf}(\cdot)$ is the error function [29, eqn. (8.250)]. Here, independent identical Gaussian distributions for the elevation and the horizontal displacement (sway) are considered, being σ_s^2 the jitter variance at the receiver. Using the previous PDFs for turbulence and misalignment fading, a closed-form expression of the combined PDF of I was derived in [39] as

$$f_I(i) = \frac{\alpha\beta\varphi^2}{A_0\Gamma(\alpha)\Gamma(\beta)} G_{1,3}^{3,0}\left(\frac{\alpha\beta}{A_0} i \,\middle|\, \begin{matrix} \varphi^2 \\ \varphi^2-1, \alpha-1, \beta-1 \end{matrix}\right), \quad i \ge 0 \tag{11}$$

where $G_{p,q}^{m,n}[\cdot]$ is the Meijer's G-function [29, eqn. (9.301)]. Even though Meijer's G-function can be expressed in terms of more familiar generalized hypergeometric functions, this PDF appears to be cumbersome to use in order to obtain simple closed-form expressions in the analysis of rate-adaptive FSO systems, leading to numerical solutions that obscure the impact of the basic system and channel parameters on performance. To overcome this inconvenience, the PDF in Eq. (11) is approximated by a single polynomial term as $f_I(i) \approx ai^b$, based on the fact that the asymptotic behavior of the system performance is dominated by the behavior of the PDF near the origin, i.e. $f_I(i)$ at $i \to 0$ determines high SNR performance [46]. Hence, using the series expansion corresponding to the Meijer's G-function [47, eqn. (07.34.06.0006.01)] and considering the fact that the two parameters α and β related to the atmospheric conditions are greater than each other, different asympotic expressions for Eq. (11), depending on the relation between the values of φ^2 and $\min\{\alpha, \beta\}$, can be written as

$$f_I(i) \approx \frac{\varphi^2(\alpha\beta)^{\min\{\alpha,\beta\}}\Gamma(|\alpha-\beta|)}{A_0^{\min\{\alpha,\beta\}}\Gamma(\alpha)\Gamma(\beta)\left(\varphi^2-\min\{\alpha,\beta\}\right)} i^{\min\{\alpha,\beta\}-1}, \quad \varphi^2 > \min\{\alpha,\beta\} \tag{12a}$$

$$f_I(i) \approx \frac{\varphi^2(\alpha\beta)^{\varphi^2}\Gamma\left(\alpha-\varphi^2\right)\Gamma\left(\beta-\varphi^2\right)}{A_0^{\varphi^2}\Gamma(\alpha)\Gamma(\beta)} i^{\varphi^2-1}, \quad \varphi^2 < \min\{\alpha,\beta\} \tag{12b}$$

It must be noted that the assumption $\alpha \neq \beta$ can be assumed under a wide variety of simulated turbulence conditions [1].

3. Error-rate performance analysis

In this section, using the previous asymptotic expressions for the combined PDF, we reveal some insights into the BER performance of rate-adaptive FSO links over atmospheric

turbulence and misalignment fading channels. We can take advantage of these simpler expressions in order to quantify the bit error-rate probability at high SNR, showing that the asymptotic performance of this metric as a function of the average SNR is characterized by two parameters: the diversity and coding gains. Assuming channel side information at the receiver, we present closed-form expressions for the average BER when the scintillation follows a gamma-gamma distribution, which cover a wide range of atmospheric turbulence conditions.

For the adaptive scheme in (3) wherein only variable silence periods are used for implementing the rate reduction and the information is detected each RR_s bit periods, the conditional BER is given by

$$P_{b_s}(E|I) = Q\left(\sqrt{RR_s^2 d^2 i^2/2N_0}\right) \tag{13}$$

where $Q(\cdot)$ is the Gaussian-Q function defined as $Q(x) = \frac{1}{\sqrt{2\pi}}\int_x^\infty e^{-\frac{t^2}{2}}dt$. Substituting the value of the Euclidean distance d gives $P_{b_s}(E|I) = Q\left(\sqrt{2\gamma\xi RR_s i}\right) = Q\left(\sqrt{2\gamma\xi\Phi_c^s i}\right)$ where $\gamma = P^2T_b/N_0$ is the average receiver SNR in the presence of the turbulence [50], knowing that PDF in (6) is normalized. It can be noted that the parameter $\Phi_c^s = RR_s$ is related to the coding gain corresponding to this rate-adaptive scheme. Hence, the average BER, $P_{b_s}(E)$, can be obtained by averaging $P_{b_s}(E|I)$ over the turbulence PDF as follows

$$P_{b_s}(E) = \int_0^\infty Q\left(\sqrt{2\gamma\xi}\Phi_c^s i\right) f_I(i)di. \tag{14}$$

In relation to the adaptive scheme in (4) wherein only repetition coding is used for implementing the rate reduction, the information is detected each bit period, combining with the same weight RR_{rc} noisy faded signals in a similar manner to a single-input multiple-output (SIMO) FSO scheme with equal gain combining (EGC) [44] and, this way, achieving a diversity gain, never greater than TDO. When TDO $>$ RR_{rc}, considering that the variance of the noise of the combined signal is $RR_{rc}N_0/2$ and substituting the value of d, the conditional BER is given by

$$P_{b_{rc}}\left(E|\{I_k\}_{k=1}^{RR_{rc}}\right) = Q\left(\sqrt{\frac{d^2}{2RR_{rc}N_0}\sum_{k=1}^{RR_{rc}} i_k}\right) = Q\left(\sqrt{\frac{2\gamma\xi}{RR_{rc}}\sum_{k=1}^{RR_{rc}} i_k}\right). \tag{15}$$

When TDO $<$ RR_{rc}, assuming for simplicity in this analysis that RR_{rc} is multiple of TDO, the conditional BER can be written as

$$P_{b_{rc}}\left(E|\{I_k\}_{k=1}^{\text{TDO}}\right) = Q\left(\sqrt{\frac{2\gamma\xi}{RR_{rc}}\frac{RR_{rc}}{\text{TDO}}\sum_{k=1}^{\text{TDO}} i_k}\right). \tag{16}$$

Both expressions can be presented in a unified way as

$$P_{b_{rc}}\left(E|\{I_k\}_{k=1}^{\Phi_d^{rc}}\right) = Q\left(\sqrt{2\gamma\xi}\Phi_c^{rc}\sum_{k=1}^{\Phi_d^{rc}} i_k\right) \tag{17}$$

where $\Phi_d^{rc} = \min\{\text{TDO}, RR_{rc}\}$, representing the diversity gain corresponding to the adaptive transmission scheme and Φ_c^{rc}, the parameter related to the coding gain corresponding to this rate-adaptive scheme, will be $\Phi_c^{rc} = 1/\sqrt{RR_{rc}}$ when $\text{TDO} \geq RR_{rc}$ and $\Phi_c^{rc} = \sqrt{RR_{rc}}/\text{TDO}$ when $\text{TDO} < RR_{rc}$. The average BER, $P_{b_{rc}}(E)$, can be obtained by averaging $P_{b_{rc}}\left(E|\{I_k\}_{k=1}^{\Phi_d^{rc}}\right)$ over the turbulence PDF as follows

$$P_{b_{rc}}(E) = \underbrace{\int_0^\infty \int_0^\infty \cdots \int_0^\infty}_{\Phi_d^{rc}\text{-fold}} Q\left(\sqrt{2\gamma\xi}\Phi_c^{rc}\sum_{k=1}^{\Phi_d^{rc}} i_k\right) \prod_{k=1}^{\Phi_d^{rc}} f_{I_k}(i_k) di_1 di_2 \ \ldots \ di_{\Phi_d^{rc}}. \tag{18}$$

From the expressions in (14) and (18), it can be deduced that a greater value for the parameter related to the coding gain using silence periods can be achieved once the whole time diversity order available in the turbulent channel by interleaving is exploited in order to achieve as much diversity gain as possible. In this way, repetition coding is firstly used in the rate-adaptive transmission proposed in (5) and then, once no more diversity gain is available, RR is increased by using variable silence periods in order to improve the coding gain. A better performance can be obtained when $\text{TDO} < RR$, being $RR = \text{TDO} \cdot RR_s$. In this way, the conditional BER is given by

$$P_{b_{rcs}}\left(E|\{I_k\}_{k=1}^{\Phi_d^{rcs}}\right) = Q\left(\sqrt{2\gamma\xi}\Phi_c^{rcs}\sum_{k=1}^{\Phi_d^{rcs}} i_k\right) \tag{19}$$

where $\Phi_d^{rcs} = \min\{\text{TDO}, RR\}$, representing the diversity gain corresponding to the rate-adaptive transmission and Φ_c^{rcs}, the parameter related to the coding gain corresponding to this rate-adaptive scheme, will be $\Phi_c^{rcs} = 1/\sqrt{RR}$ when $\text{TDO} \geq RR$, as in repetition coding, and $\Phi_c^{rcs} = RR_s/\sqrt{\text{TDO}}$ when $\text{TDO} < RR$, a greater value than Φ_c^{rc}. Hence, the average BER, $P_{b_{rcs}}(E)$, can be obtained by averaging $P_{b_{rcs}}\left(E|\{I_k\}_{k=1}^{\Phi_d^{rcs}}\right)$ over the turbulence PDF as follows

$$P_{b_{rcs}}(E) = \underbrace{\int_0^\infty \int_0^\infty \cdots \int_0^\infty}_{\Phi_d^{rcs}\text{-fold}} Q\left(\sqrt{2\gamma\xi}\Phi_c^{rcs}\sum_{k=1}^{\Phi_d^{rcs}} i_k\right) \prod_{k=1}^{\Phi_d^{rcs}} f_{I_k}(i_k) di_1 di_2 \ \ldots \ di_{\Phi_d^{rcs}}. \tag{20}$$

Finally, the average BER corresponding to the three previous rate-adaptive transmission schemes can be written in a unified way as

$$P_b(E) = \int_0^\infty Q\left(\sqrt{2\gamma\xi}\Phi_c i\right) f_{I_T}(i) di \tag{21}$$

where I_T represents the sum of variates $I_T = \sum_{k=1}^{\Phi_d} I_k$ whose PDF is given by $f_{I_T}(i)$, Φ_c represents the parameter related to the coding gain, being equal to Φ_c^s, Φ_c^{rc} and Φ_c^{rcs}, respectively, and Φ_d represents the diversity gain, i.e. the slope of the BER versus average SNR, being equal to 1, Φ_d^{rc} and Φ_d^{rcs}, respectively. Since the variates are independent, knowing that the resulting PDF of their sum is the convolution of their corresponding PDFs, obtained via single-sided Laplace

and its inverse transforms, approximate expressions for the PDF, $f_{I_T}(i)$, of the combined variate can be easily derived as

$$f_{I_T}(i) \approx \frac{1}{\Gamma(\Phi_d \Omega_{min})} \left(\frac{(\alpha\beta)^{\Omega_{min}} \varphi^2 \Gamma(|\alpha - \beta|)}{A_0^{\Omega_{min}} \Gamma(\Omega_{max}) (\varphi^2 - \Omega_{min})} \right)^{\Phi_d} i^{\Phi_d \Omega_{min} - 1}, \quad \varphi^2 > \Omega_{min} \tag{22a}$$

$$f_{I_T}(i) \approx \frac{1}{\Gamma(\Phi_d \varphi^2)} \left(\frac{(\alpha\beta)^{\varphi^2} \Gamma(\alpha - \varphi^2) \Gamma(\beta - \varphi^2) \Gamma(1 + \varphi^2)}{A_0^{\varphi^2} \Gamma(\alpha) \Gamma(\beta)} \right)^{\Phi_d} i^{\Phi_d \varphi^2 - 1}, \quad \varphi^2 < \Omega_{min} \tag{22b}$$

where $\Omega_{min} = \min\{\alpha, \beta\}$ and $\Omega_{max} = \max\{\alpha, \beta\}$ are used for readability. To evaluate the integral in Eq. (21), we can use that the Q-function is related to the complementary error function $\text{erfc}(\cdot)$ by $\text{erfc}(x) = 2Q(\sqrt{2}x)$ [29, eqn. (6.287)] and the fact that $\int_0^\infty \text{erfc}(x) x^{a-1} dx = \Gamma((1+a)/2)/(\pi^{1/2} a)$ [29, eqn. (6.281)], obtaining the corresponding closed-form asymptotic solutions for the BER as can be seen in

$$P_b(E) \doteq \left(\left(\frac{A_0^{-\Omega_{min}} (\alpha\beta)^{\Omega_{min}} \varphi^2 \Gamma(|\alpha - \beta|) (\Gamma(\Omega_{max}))^{-1}}{\left(2\Gamma\left(1 + \frac{\Phi_d \Omega_{min}}{2}\right)\right)^{1/\Phi_d} (-\Omega_{min} + \varphi^2)} \right)^{-\frac{2}{\Omega_{min}}} 4\Phi_c^2 \gamma\xi \right)^{-\frac{\Phi_d \Omega_{min}}{2}}, \quad \varphi^2 > \Omega_{min} \tag{23a}$$

$$P_b(E) \doteq \left(\left(\frac{(\alpha\beta)^{\varphi^2} \Gamma\left(\alpha - \varphi^2\right) \Gamma\left(\beta - \varphi^2\right) \Gamma(1 + \varphi^2)}{A_0^{\varphi^2} \left(2\Gamma\left(1 + \frac{\Phi_d \varphi^2}{2}\right)\right)^{1/\Phi_d} \Gamma(\alpha) \Gamma(\beta)} \right)^{-\frac{2}{\varphi^2}} 4\Phi_c^2 \gamma\xi \right)^{-\frac{\Phi_d \varphi^2}{2}}, \quad \varphi^2 < \Omega_{min} \tag{23b}$$

The results corresponding to this FSO scenario are illustrated in the Fig. 2, when different levels of turbulence strength of $(\alpha, \beta) = (4, 2)$ and $(\alpha, \beta) = (2, 1)$ are assumed together with values of normalized jitter of $\sigma_s/r = \{1, 3\}$ and a normalized beamwidth of $\omega_z/r = \{5, 10\}$, corresponding to values of scintillation index of $SI = 0.875$ and $SI = 2$, respectively. Here, rectangular pulse shapes with $\xi = 1$ are used for values of TDO $= \{1, 2, 4\}$, rate reductions of $RR = \{1, 2, 4, 8\}$ and the three rate-adaptive transmission schemes presented in the previous section, based on: the only use of silence periods (Sil), the only use of repetition coding (Rep) and, finally, the joint use of repetition codes and variable silence periods (Rep&Sil). Monte Carlo simulation results are furthermore included as a reference, confirming the accuracy and usefulness of the derived results. Due to the long simulation time involved, simulation results only up to BER=10^{-8} are included. Simulation results corroborate that asymptotic expressions here obtained lead to simple bounds on the bit error probability that get tighter over a wider range of SNR as the turbulence strength increases. In particular, Eq. (23*a*) is corroborated in this figure since $\varphi^2 > \Omega_{min}$ is satisfied when values of $(\omega_z/r, \sigma_s/r) = (5, 1)$ and $(\omega_z/r, \sigma_s/r) = (10, 3)$ are assumed. It is straightforward to show that the average BER behaves asymptotically as $(G_c \gamma\xi)^{-G_d}$, where G_d and G_c denote diversity order and coding gain, respectively [40, 46]. At high SNR, if asymptotically the error probability behaves as $(G_c \gamma\xi)^{-G_d}$, the diversity order G_d determines the slope of the BER versus average SNR curve in a log-log scale and the coding gain G_c (in decibels) determines the shift of the curve in SNR.

In the same way, Eq. (23*b*) is corroborated in Fig. 3 when $(\alpha, \beta) = (4, 2)$ is assumed together with values of normalized jitter of $\sigma_s/r = \{1, 4\}$ and a normalized beamwidth of $\omega_z/r = 5$.

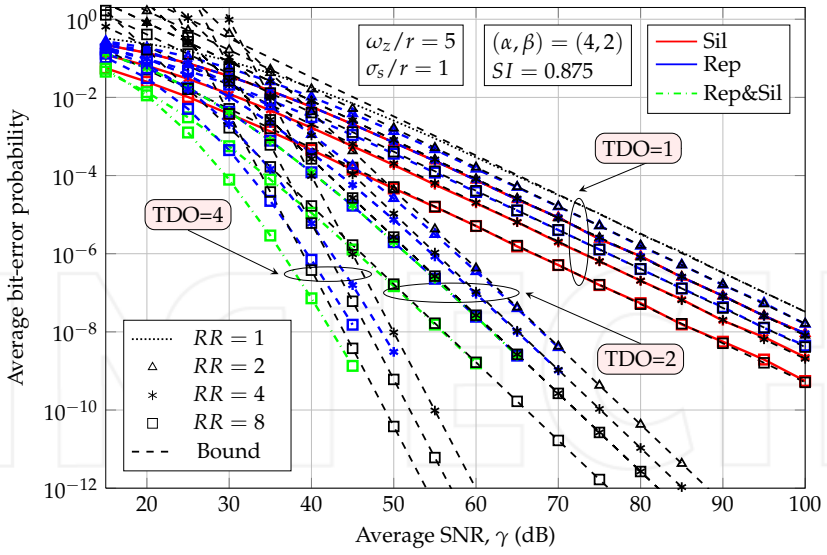

(a)

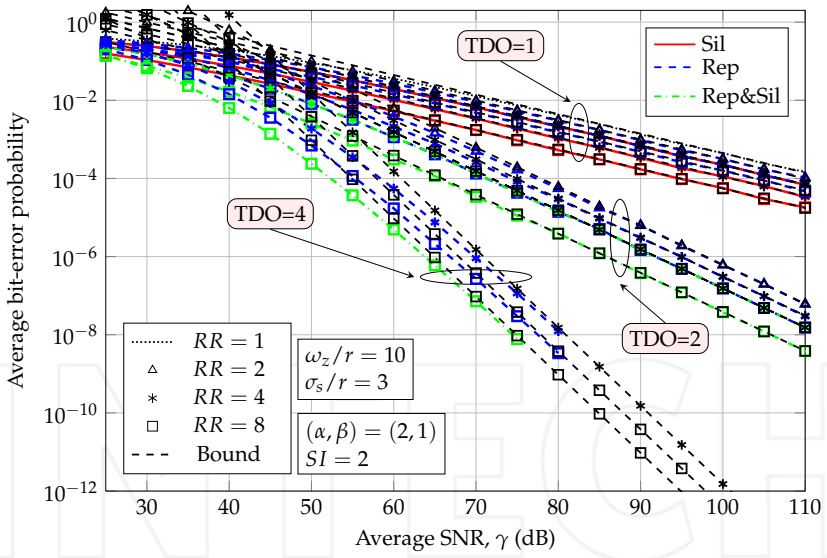

(b)

Figure 2. BER performance in FSO IM/DD links using different rate-adaptive transmission schemes over gamma-gamma atmospheric and misalignment fading channels, when different levels of turbulence (a) $(\alpha, \beta) = (5, 1)$, (b) $(\alpha, \beta) = (10, 3)$ are assumed together with values of normalized jitter of $\sigma_s/r = \{1, 3\}$ and a normalized beamwidth of $\omega_z/r = \{5, 10\}$.

Here, rectangular pulse shapes with $\xi = 1$ are used for values of TDO $= \{2, 4\}$, rate reductions of $RR = \{2, 4, 8\}$ and rate-adaptive transmission schemes presented in the previous section, based on: the only use of repetition coding (Rep) and the joint use of repetition codes and variable silence periods (Rep&Sil). It can be noted that the bound corresponding to Eq. $(23b)$ is displayed in this figure when $\sigma_s/r = 4$ is considered since $\varphi^2 < \Omega_{min}$ is satisfied, showing lower performance due to the diversity order is determined by the pointing errors. At this

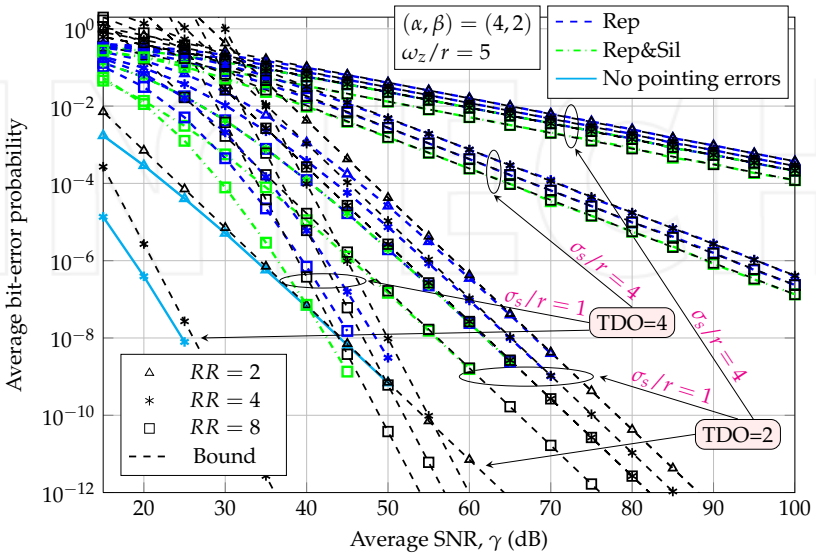

Figure 3. BER performance in FSO IM/DD links using different rate-adaptive transmission schemes over gamma-gamma atmospheric channels with/without pointing errors, assuming TDO$= \{2, 4\}$ and values of normalized jitter of $\sigma_s/r = \{1, 4\}$ and normalized beamwidth of $\omega_z/r = 5$.

point, it can be convenient to compare with the BER performance obtained in a similar context when misalignment fading is not present. Knowing that the impact of pointing errors in our analysis can be suppressed by assuming $A_0 \to 1$ and $\varphi^2 \to \infty$ [16], the corresponding asymptotic expression can be easily derived from Eq. $(23a)$ as follows

$$P_b(E) \doteq \left(\left(\frac{(\alpha\beta)^{\Omega_{min}} \Gamma\left(|\alpha - \beta|\right) \left(\Gamma(\Omega_{max})\right)^{-1}}{\left(2\Gamma\left(1 + \frac{\Phi_d \Omega_{min}}{2}\right)\right)^{1/\Phi_d}} \right)^{-\frac{2}{\Omega_{min}}} 4\Phi_c^2 \gamma \xi \right)^{-\frac{\Phi_d \Omega_{min}}{2}} \tag{24}$$

In Fig. 3, BER performance in FSO links using different rate-adaptive transmission schemes over gamma-gamma atmospheric channels with/without pointing errors is displayed, exploiting a potential time-diversity order available in the turbulent channel of 2 and 4, and values of σ_s/r of 1 and 4 with normalized beamwidth of $\omega_z/r = 5$, where a turbulence strength of $(\alpha, \beta) = (4, 2)$ has been assumed. From this asymptotic analysis, it can be deduced that the main aspect to consider in order to optimize the error-rate performance is the relation between the values of φ^2 and $\min\{\alpha, \beta\}$. So, it is shown that the diversity order is independent of the pointing errors when the equivalent beam radius at the receiver is at least

$2(\min\{\alpha,\beta\})^{1/2}$ times the value of the pointing error displacement standard deviation at the receiver. Once this condition is satisfied, taking into account the coding gain in Eq. $(23a)$, the impact of the pointing error effects translates into a coding gain disadvantage, $D[dB]$, relative to gamma-gamma atmospheric turbulence without misalignment fading given by

$$D[dB] \triangleq \frac{20}{\Omega_{min}} \log_{10}\left(\frac{\varphi^2}{A_0^{\Omega_{min}}(\varphi^2-\Omega_{min})}\right). \tag{25}$$

In a similar way as in the outage and error rate performance analysis of MIMO FSO links [21, 25], it is also here corroborated that the impact of pointing errors is not related to the rate-adaptive scheme, obtaining the same coding gain disadvantage regardless the rate reduction. According to this expression, it can be observed in Fig. 3 that a coding gain disadvantage of 23.9 decibels is achieved for a value of $(\omega_z/r, \sigma_s/r) = (5,1)$, for both a rate reduction of $RR = 2$ and $RR = 4$.

Additionally, as previously reported by the authors [25, 26], a relevant improvement in performance must be noted as a consequence of the pulse shape used, providing an increment in the average SNR of $10\log_{10}\xi$ decibels. This superiority has been previously reported by the authors in terms of closed-form expressions corresponding to the average BER performance in several FSO scenarios [19, 24, 26], as well as from the point of view of information theory [22]. Following the approach here presented, this improvement can be viewed as an additional coding gain, regardless of the rate-adaptive transmission scheme employed. So, for instance, when a rectangular pulse shape of duration κT_b, with $0 < \kappa \leq 1$, is adopted, a value of $\xi = 1/\kappa$ can be easily shown. Nonetheless, a significantly higher value of $\xi = 4/\kappa\sqrt{\pi}$ is obtained when a Gaussian pulse of duration κT_b as $g(t) = \exp\left(-t^2/2\rho^2\right)\ \forall |t| < \kappa T_b/2$ is adopted, where $\rho = \kappa T_b/8$ and the reduction of duty cycle is also here controlled by the parameter κ. In this fashion, 99.99% of the average optical power of a Gaussian pulse shape is being considered. Ultrashort pulses from mode-locked lasers often have a temporal shape which can be described with a Gaussian function. This improvement in performance due to the pulse shape can be even increased when a squared hyperbolic secant (sech^2) function is employed which is another temporal shape proper to ultrashort pulses from mode-locked lasers [11]. In this way, a value of $\xi = 8/3\kappa$, greater than that of the Gaussian pulse, is obtained when a sech^2 pulse of duration κT_b as $g(t) = \text{sech}^2\left(t/\rho\right)\ \forall |t| < \kappa T_b/2$ is adopted, where $\rho = \kappa T_b/8$ and the reduction of duty cycle is also here controlled by the parameter κ. As in previous pulse shape, 99.99% of the average optical power of a sech^2 pulse shape is being considered. Obtained results corresponding to the sech^2 pulse shape with $\kappa = 0.25$ for the rate-adaptive transmission (Rep&Sil) here proposed with $\text{TDO} = 2$ and rate reductions of $RR = \{1,2,4,8\}$ are displayed in Fig. 4 together with results previously displayed in Fig. 2(a) where rectangular pulse shapes with $\kappa = 1$ are used. From this figure, it can be observed that a significant horizontal shift in the BER performance above 10 decibels is achieved in any case, regardless of the rate reduction assumed.

4. Achievable information rate performance analysis

In this section, the analysis of the achievable information rate corresponding to the three rate-adaptive transmission schemes here presented is considered. From the mode of operation based on reducing the initial rate, $R_b = 1/T_b$, for a RR parameter as R_b/RR in order to achieve

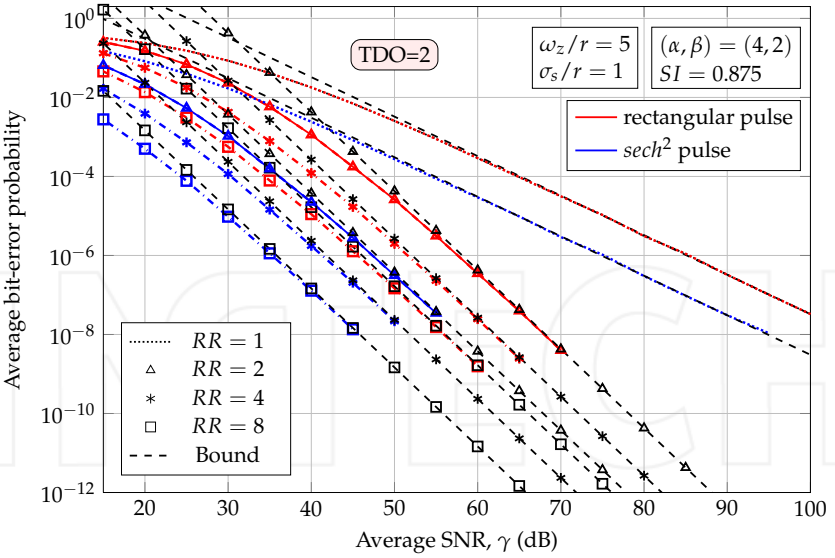

Figure 4. Performance of the sech^2 pulse shape with $\kappa = 0.25$ for the rate-adaptive scheme (Rep&Sil) with TDO $= 2$ and $RR = \{1, 2, 4, 8\}$ in FSO IM/DD links over gamma-gamma atmospheric channels with pointing errors, assuming a value of normalized jitter of $\sigma_s/r = 1$ and normalized beamwidth of $\omega_z/r = 5$.

a target BER requirement P_b, the achievable information rate, R, in bits/channel use, can be defined as $R = 1/RR$. While the required value of RR to satisfy a target BER requirement can be numerically solved from analytical results in (21), we can significantly simplify this analysis when target BER requirements and levels of turbulence imply a sufficiently tight performance for the corresponding asymptotic BER in (23). From results displayed in Fig. 2, it can be deduced that the asymptotic BER expressions are closer and closer upper bounds for the BER performance as the level of turbulence is increased. This is an expected conclusion since a greater value of average SNR is required to satisfy the same predefined target BER requirement. In this sense, making use of the asymptotic BER in (23*a*), the achievable information rate can be written as

$$R_{Sil}(\gamma) = \left(\frac{2^{\Omega_{min}} A_0^{\Omega_{min}} P_b \Omega_{min} (\xi\gamma)^{\Omega_{min}/2} \left(\varphi^2 - \Omega_{min}\right) \Gamma(\Omega_{max}) \Gamma\left(\Omega_{min}/2\right)}{\varphi^2 (\alpha\beta)^{\Omega_{min}} \Gamma(|\alpha - \beta|)} \right)^{1/\Omega_{min}} \tag{26}$$

$$R_{Rep}(\gamma) = \left(\frac{\mathrm{TDO}^{-\Omega_{min}} A_0^{\Omega_{min}} \Gamma(\Omega_{max}) \left(\varphi^2 - \Omega_{min}\right) (4\gamma\xi)^{\Omega_{min}/2}}{\varphi^2 (\alpha\beta)^{\Omega_{min}} \Gamma(|\alpha - \beta|) \left(2P_b \Gamma\left(\frac{\mathrm{TDO}\Omega_{min}}{2} + 1\right)\right)^{-1/\mathrm{TDO}}} \right)^{2/\Omega_{min}} \tag{27}$$

$$R_{Rep\&Sil}(\gamma) = \left(\frac{\mathrm{TDO}^{-3\Omega_{min}/2} A_0^{\Omega_{min}} \Gamma(\Omega_{max}) \left(\varphi^2 - \Omega_{min}\right) (4\gamma\xi)^{\Omega_{min}/2}}{\varphi^2 (\alpha\beta)^{\Omega_{min}} \Gamma(|\alpha - \beta|) \left(2P_b \Gamma\left(\frac{\mathrm{TDO}\Omega_{min}}{2} + 1\right)\right)^{-1/\mathrm{TDO}}} \right)^{1/\Omega_{min}} \tag{28}$$

for the rate-adaptive transmission schemes Sil, Rep and Rep&Sil, respectively. It can

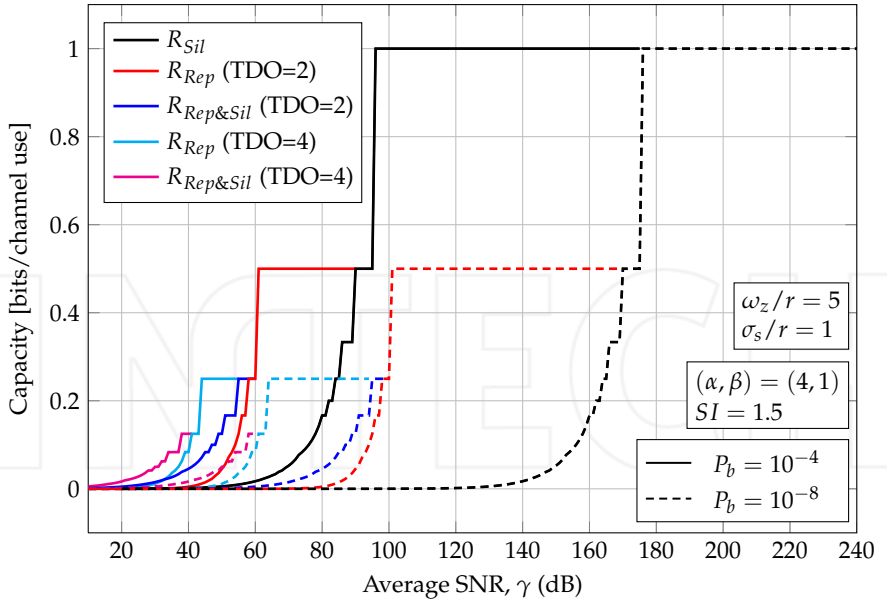

(a)

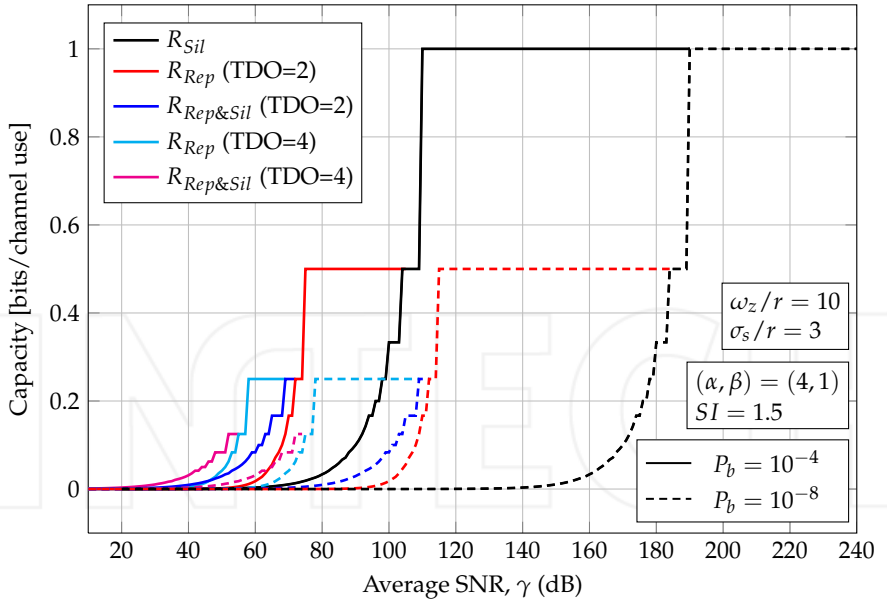

(b)

Figure 5. Achievable information rate in FSO IM/DD links corresponding to the rate-adaptive transmission schemes Sil, Rep and Rep&Sil over gamma-gamma atmospheric and misalignment fading channels for two different target BER requirements, $P_b = 10^{-4}$ and $P_b = 10^{-8}$, and time-diversity orders of TDO=$\{2, 4\}$. Here, $(\alpha, \beta) = (4, 1)$ is assumed together with values of normalized jitter and normalized beamwidth of (a) $(\omega_z/r, \sigma_s/r) = (5, 1)$ and (b) $(\omega_z/r, \sigma_s/r) = (10, 3)$.

be observed that the rate-adaptive scheme Sil does not take advantage of the potential time-diversity order available in the turbulent channel. The achievable information rate in (26), (27) and (28) is depicted in Fig. 5, corresponding to the rate-adaptive transmission schemes Sil, Rep and Rep&Sil, respectively, for two different target BER requirements, $P_b = 10^{-4}$ and $P_b = 10^{-8}$, and TDO=$\{2, 4\}$. It can be noted that obtained results are in excellent agreement with previous results presented in terms of BER performance in Fig. 2. In this sense, it can be observed that the required value of SNR to satisfy a target BER is greater when the impact of pointing errors is more severe, even when the same level of atmospheric turbulence strength is considered.

From this figure, it can be deduced not only the superiority of the rate-adaptive transmission scheme based on the joint use of repetition coding and variable silence periods but also that an adaptive transmission design approach based on taking advantage out of the potential time-diversity order available in the turbulent channel is required, corroborating the fact that the rate-adaptive transmission scheme only based on variable silence periods implies a remarkably inefficient performance from the point of view of information theory. In this way, it can be observed that even when the available time-diversity order is low (TDO=2) a relevant improvement in achievable information rate is obtained, especially when a lower target BER is demanded. In spite of high values of TDO cannot be possible because of the latency introduced by the interleaver, to achieve a time diversity order available of TDO=2, perfect interleaving can be done by simply sending the same information delayed by the expected fade duration, as shown experimentally in [32] for a rate reduction of 2. It must be commented that the rate-adaptive transmission scheme proposed is not based on an adaptive signal constellation where more complicated modulation techniques can be defined, being assumed the use of OOK signaling due to its simplicity and low implementation cost, and, hence, an achievable information rate not higher than 1 bit/channel use can be achieved, since this is determined by the signal constellation and how the coding technique is able to take advantage of it. At the expense of a greater simplicity in hardware implementation, lower values of capacity are achieved if compared to rate-adaptive transmission schemes based on adaptive modulation or coding techniques more sophisticated than repetition coding and the inclusion of variable silence periods [10, 12, 14].

5. Conclusions

In this chapter, a simple rate-adaptive transmission scheme for FSO communication systems with intensity modulation and direct detection over atmospheric turbulence channels with pointing errors is analyzed. This scheme is based on the joint use of repetition coding and variable silence periods, exploiting the potential time-diversity order available in the turbulent channel as well as allowing the increase of the PAOPR, which has shown to be a favorable characteristic in IM/DD FSO links [19, 24, 26]. Here, repetition coding is firstly used in order to accomodate the transmission rate to the channel conditions until the whole time diversity order available in the turbulent channel by interleaving is exploited. Then, once no more diversity gain is available, the rate reduction can be increased by using variable silence periods in order to increase the PAOPR. Novel closed-form asymptotic expressions are derived when the irradiance of the transmitted optical beam is susceptible to either a wide range of turbulence conditions (weak to strong), following a gamma-gamma distribution of parameters α and β, or pointing errors, following a misalignment fading model, as in [16–18, 38], where the effect of beam width, detector size and jitter variance is considered.

Furthermore, we extend the concepts of diversity and coding gain, which are well known from the RF communication literature [40], to the rate-adaptive FSO systems under study, allowing us to provide simple, insightful, and accurate closed-form approximations for the BER performance at high SNR. Simulation results are further demonstrated to confirm the analytical results. Here, not only rectangular pulses are considered but also OOK formats with any pulse shape, corroborating the advantage of using pulses with high PAOPR, such as Gaussian pulses or squared hyperbolic secant pulses, and concluding the fact that this improvement can be viewed as an additional coding gain, regardless of the rate-adaptive scheme employed or even in absence of rate-adaptive transmission.

In terms of pros and cons of using the adaptive transmission scheme Rep&Sil here analyzed and proposed, we can conclude that one of the pros of this adaptive transmission scheme is the greater simplicity, requiring a lower implementation complexity if compared to alternative rate-adaptive transmission schemes proposed for use in FSO systems [10, 12, 14, 34]. In this sense, the use of OOK signaling with repetition coding implies a hardware implementation of a significant lower complexity if compared to that required by the variable rate turbo-coding scheme as proposed in [34], the adaptive LDPC-coded modulation and transmission scheme that varied both the power and the modulation order of a FSO system with M-ary pulse amplitude modulation as proposed in [12, 14] and the adaptive transmission techniques employing subcarrier phase shift keying intensity modulation as proposed in [10]. Additionally, together with the use of repetition coding, the adaptive scheme Rep&Sil here proposed considers the inclusion of variable silence periods once no more diversity gain is available, providing a higher level of PAOPR and, hence, a better performance, without the need of increasing complexity in hardware implementation. On the contrary, one of the cons of the rate-adaptive transmission scheme here proposed in relation to previous rate-adaptive transmission schemes is the lower capacity achieved since no adaptive modulation is considered, proposing the use of OOK signaling due to its simplicity and low implementation cost and, hence, providing an achievable information rate not higher than 1 bit/channel use.

Acknowledgments

The authors are grateful for financial support from the Junta de Andalucía (research group "Communications Engineering (TIC-0102)").

Author details

Antonio García-Zambrana and Beatriz Castillo-Vázquez
Department of Communications Engineering, University of Málaga, Spain

Carmen Castillo-Vázquez
Department of Statistics and Operations Research, University of Málaga, E-29071 Málaga, Spain

6. References

[1] Al-Habash, M. A., Andrews, L. C. & Phillips, R. L. [2001]. Mathematical model for the irradiance probability density function of a laser beam propagating through turbulent media, *Opt. Eng.* 40: 8.

[2] Ali, A. A. & Al-Kadi, I. A. [1989]. On the use of repetition coding with binary digital modulations on mobile channels, *IEEE Trans. Veh. Technol.* 38(1): 14–18.
[3] Andrews, L., Phillips, R. & Hopen, C. [2001]. *Laser beam scintillation with applications*, Bellingham, WA: SPIE Press.
[4] Anguita, J., Djordjevic, I., Neifeld, M. & Vasic, B. [2005]. Shannon capacities and error-correction codes for optical atmospheric turbulent channels, *J. Opt. Netw.* 4(9): 586–601.
[5] Arnon, S. [2003]. Effects of atmospheric turbulence and building sway on optical wireless-communication systems, *Opt. Lett.* 28(2): 129–131.
[6] Bayaki, E. & Schober, R. [2010]. On space-time coding for free-space optical systems, *IEEE Trans. Commun.* 58(1): 58–62.
[7] Bayaki, E., Schober, R. & Mallik, R. K. [2009]. Performance analysis of mimo free-space optical systems in gamma-gamma fading, *IEEE Trans. Commun.* 57(11): 3415–3424.
[8] Borah, D. K. & Voelz, D. G. [2009]. Pointing error effects on free-space optical communication links in the presence of atmospheric turbulence, *J. Lightwave Technol.* 27(18): 3965–3973.
[9] Chan, V. W. S. [2006]. Free-space optical communications, *J. Lightwave Technol.* 24(12): 4750–4762.
[10] Chatzidiamantis, N. D., Lioumpas, A. S., Karagiannidis, G. K. & Arnon, S. [2011]. Adaptive subcarrier PSK intensity modulation in free space optical systems, *IEEE Trans. Commun.* 59(5): 1368–1377.
[11] Diels, J. C. & Rudolph, W. [2006]. *Ultrashort Laser Pulse Phenomena*, Optics and Photonics Series, second edn, Academic Press.
[12] Djordjevic, I. B. [2010]. Adaptive modulation and coding for free-space optical channels, *IEEE/OSA Journal of Optical Communications and Networking* 2(5): 221–229.
[13] Djordjevic, I. B., Denic, S., Anguita, J., Vasic, B. & Neifeld, M. [2008]. Ldpc-coded mimo optical communication over the atmospheric turbulence channel, *J. Lightwave Technol.* 26(5): 478–487.
[14] Djordjevic, I. B. & Djordjevic, G. T. [2009]. On the communication over strong atmospheric turbulence channels by adaptive modulation and coding, *Opt. Express* 17(20): 18250–18262.
[15] Fante, R. L. [1975]. Electromagnetic beam propagation in turbulent media, *Proc. IEEE* 63(12): 1669–1692.
[16] Farid, A. A. & Hranilovic, S. [2007]. Outage capacity optimization for free-space optical links with pointing errors, *J. Lightwave Technol.* 25(7): 1702–1710.
[17] Farid, A. A. & Hranilovic, S. [2010]. Diversity gains for mimo wireless optical intensity channels with atmospheric fading and misalignment, *Proc. IEEE GLOBECOM Workshops (GC Wkshps)*, pp. 1015–1019.
[18] Gappmair, W., Hranilovic, S. & Leitgeb, E. [2010]. Performance of ppm on terrestrial fso links with turbulence and pointing errors, *IEEE Commun. Lett.* 14(5): 468–470.
[19] García-Zambrana, A. [2007]. Error rate performance for STBC in free-space optical communications through strong atmospheric turbulence, *IEEE Commun. Lett.* 11(5): 390–392.
[20] García-Zambrana, A., Castillo-Vázquez, B. & Castillo-Vázquez, C. [2010a]. Average capacity of FSO links with transmit laser selection using non-uniform OOK signaling over exponential atmospheric turbulence channels, *Opt. Express* 18(19): 20445–20454.

[21] García-Zambrana, A., Castillo-Vázquez, B. & Castillo-Vázquez, C. [2012]. Asymptotic error-rate analysis of fso links using transmit laser selection over gamma-gamma atmospheric turbulence channels with pointing errors, *Opt. Express* 20(3): 2096–2109.

[22] García-Zambrana, A., Castillo-Vázquez, C. & Castillo-Vázquez, B. [2010b]. On the capacity of FSO links over gamma-gamma atmospheric turbulence channels using OOK signaling, *EURASIP Journal on Wireless Communications and Networking* . Article ID 127657, 9 pages, 2010. doi:10.1155/2010/127657.

[23] García-Zambrana, A., Castillo-Vázquez, C. & Castillo-Vázquez, B. [2010c]. Rate-adaptive FSO links over atmospheric turbulence channels by jointly using repetition coding and silence periods, *Opt. Express* 18(24): 25422–25440.

[24] García-Zambrana, A., Castillo-Vázquez, C. & Castillo-Vázquez, B. [2010d]. Space-time trellis coding with transmit laser selection for FSO links over strong atmospheric turbulence channels, *Opt. Express* 18(6): 5356–5366.

[25] García-Zambrana, A., Castillo-Vázquez, C. & Castillo-Vázquez, B. [2011]. Outage performance of MIMO FSO links over strong turbulence and misalignment fading channels, *Opt. Express* 19(14): 13480–13496.

[26] Garcia-Zambrana, A., Castillo-Vazquez, C., Castillo-Vazquez, B. & Hiniesta-Gomez, A. [2009]. Selection transmit diversity for FSO links over strong atmospheric turbulence channels, *IEEE Photon. Technol. Lett.* 21(14): 1017–1019.

[27] García-Zambrana, A. & Puerta-Notario, A. [1999]. RZ-Gaussian pulses reduce the receiver complexity in wireless infrared links at high bit rates, *IEE Electronics Letters* 35(13): 1059–1061.

[28] García-Zambrana, A. & Puerta-Notario, A. [2001]. Large change rate-adaptive indoor wireless infrared links using variable silence periods, *IEE Electronics Letters* 37(8): 524–525.

[29] Gradshteyn, I. S. & Ryzhik, I. M. [2007]. *Table of integrals, series and products*, 7th edn, Academic Press Inc.

[30] Hranilovic, S. & Kschischang, F. R. [2003]. Optical intensity-modulated direct detection channels: signal space and lattice codes, *IEEE Trans. Inf. Theory* 49(6): 1385–1399.

[31] Kahn, J. M. & Barry, J. R. [1997]. Wireless infrared communications, *Proc. IEEE* 85: 265–298.

[32] Kwok, C. H., Penty, R. V. & White, I. H. [2008]. Link reliability improvement for optical wireless communication systems with temporal-domain diversity reception, *IEEE Photon. Technol. Lett.* 20(9): 700–702.

[33] Lee, E. J. & Chan, V. W. S. [2004]. Part 1: optical communication over the clear turbulent atmospheric channel using diversity, *IEEE J. Sel. Areas Commun.* 22(9): 1896–1906.

[34] Li, J. & Uysal, M. [2003]. Achievable information rate for outdoor free space optical communication with intensity modulation and direct detection, *Proc. IEEE Global Telecommunications Conference GLOBECOM '03*, Vol. 5, pp. 2654–2658.

[35] Lim, W., Yun, C. & Kim, K. [2009]. Ber performance analysis of radio over free-space optical systems considering laser phase noise under gamma-gamma turbulence channels, *Opt. Express* 17(6): 4479–4484.

[36] Liu, C., Yao, Y., Sun, Y. X., Xiao, J. J. & Zhao, X. H. [2010]. Average capacity optimization in free-space optical communication system over atmospheric turbulence channels with pointing errors, *Opt. Lett.* 35(19): 3171–3173.

[37] Nistazakis, H. E., Karagianni, E. A., Tsigopoulos, A. D., Fafalios, M. E. & Tombras, G. S. [2009]. Average capacity of optical wireless communication systems over atmospheric turbulence channels, *IEEE/OSA Journal of Lightwave Technology* 27(8): 974–979.
[38] Sandalidis, H. G. [2011]. Coded free-space optical links over strong turbulence and misalignment fading channels, *IEEE Trans. Commun.* 59(3): 669–674.
[39] Sandalidis, H. G., Tsiftsis, T. A. & Karagiannidis, G. K. [2009]. Optical wireless communications with heterodyne detection over turbulence channels with pointing errors, *J. Lightwave Technol.* 27(20): 4440–4445.
[40] Simon, M. K. & Alouini, M.-S. [2005]. *Digital communications over fading channels*, second edn, Wiley-IEEE Press, New Jersey.
[41] Stotts, L. B., Andrews, L. C., Cherry, P. C., Foshee, J. J., Kolodzy, P. J., McIntire, W. K., Northcott, M., Phillips, R. L., Pike, H. A., Stadler, B. & Young, D. W. [2009]. Hybrid optical rf airborne communications, *Proc. IEEE* 97(6): 1109–1127.
[42] Trisno, S., Smolyaninov, I. I., Milner, S. D. & Davis, C. C. [2004]. Delayed diversity for fade resistance in optical wireless communication system through simulated turbulence, *Proc. SPIE*, pp. 385–394.
[43] Trisno, S., Smolyaninov, I. I., Milner, S. D. & Davis, C. C. [2005]. Characterization of delayed diversity optical wireless system to mitigate atmospheric turbulence induced fading, *Proc. SPIE*, pp. 589215.1–589215.10.
[44] Tsiftsis, T. A., Sandalidis, H. G., Karagiannidis, G. K. & Uysal, M. [2009]. Optical wireless links with spatial diversity over strong atmospheric turbulence channels, *IEEE Trans. Wireless Commun.* 8(2): 951–957.
[45] Uysal, M., Li, J. & Yu, M. [2006]. Error rate performance analysis of coded free-space optical links over gamma-gamma atmospheric turbulence channels, *IEEE Trans. Wireless Commun.* 5(6): 1229–1233.
[46] Wang, Z. & Giannakis, G. B. [2003]. A simple and general parameterization quantifying performance in fading channels, *IEEE Trans. Commun.* 51(8): 1389–1398.
[47] Wolfram Research, Inc. [n.d.]. The Wolfram functions site.
URL: *http://functions.wolfram.com*
[48] Xu, F., Khalighi, A., Caussé, P. & Bourennane, S. [2009]. Channel coding and time-diversity for optical wireless links, *Opt. Express* 17(2): 872–887.
[49] Young, C. Y., Andrews, L. C. & Ishimaru, A. [1998]. Time-of-arrival fluctuations of a space–time gaussian pulse in weak optical turbulence: an analytic solution, *Appl. Opt.* 37(33): 7655–7660.
[50] Zhu, X. & Kahn, J. M. [2002]. Free-space optical communication through atmospheric turbulence channels, *IEEE Trans. Commun.* 50(8): 1293–1300.